

## Pharmacophore Modeling of Tyrosine Kinase Inhibitors: 4-Anilinoquinazoline Derivatives

Yeong-Sheng Chang<sup>a</sup> (張詠昇), Ling-Ling Yang<sup>b,\*</sup> (楊玲玲) and Bo-Cheng Wang<sup>a,\*</sup> (王伯昌)

<sup>a</sup>Department of Chemistry, Tamkang University, Taipei 251, Taiwan, R.O.C.

<sup>b</sup>Graduate Institute of Pharmacognosy Science, Taipei Medical University, Taipei 116, Taiwan, R.O.C.

A pharmacophore model for the inhibition of Tyrosine Kinase is established that could serve as a guide for the rational design of high potent and selective inhibitors. Recently, quantitative structure-activity relationships for 4-anilinoquinazoline class of inhibitors to inhibit EGFR autophosphorylation are in great demand. We have developed a quantitatively predictive chemical function-based pharmacophore model by using Discovery Studio 2.1 software. The optimal hypothesis consists of four features: three hydrophobic (HYD), and one hydrogen bond donor (HBD) functions. The input for HypoGen was a training set of 16 compounds exhibiting IC<sub>50</sub> values ranging between 0.025 nM and 12000 nM, and having the output borne significant conventional coefficient of 0.97. To further validate our design rationale, protein-ligand docking software was used to elucidate the intra-molecular interactions. Therefore, the established pharmacophore model could help to a better understanding on how the substituents might influence the activity and afford important information for both ligand-based and structure-based drug designs.

**Keywords:** Pharmacophore model; Tyrosine kinase; Quantitative structure-activity relationship; 4-Anilinoquinazoline; EGFR; HypoGen.

### INTRODUCTION

The protein phosphorylation is a critical mechanism for regulating protein function in many cell regulatory processes.<sup>1</sup> Recently, the growth factor signaling pathways are the main focus of research for the novel cancer chemotherapy (e.g. breast, lung, colon, and prostate) because of their fundamental role in regulating key cellular functions which include cell proliferation, differentiation, metastasis and survival.<sup>2-4</sup> An important mediator of growth factor signaling pathways is the epidermal growth factor receptor (EGFR). It has been illustrated that small molecules can selectively inhibit the EGFR, and they have a great therapeutic potential in the treatment of malignant and nonmalignant epithelial diseases.

Of several candidate compounds synthesized and tested, gefitinib (1) was the first EGFR-tyrosine kinase inhibitor being approved by US FDA (Food and Drug Administration) for the treatment of non-small cell lung cancer, and later erlotinib (2), which belongs to same class, and was used following a prior chemotherapeutic intervention. In 2007, Lapatinib (3) (Fig. 1) was approved by US FDA to

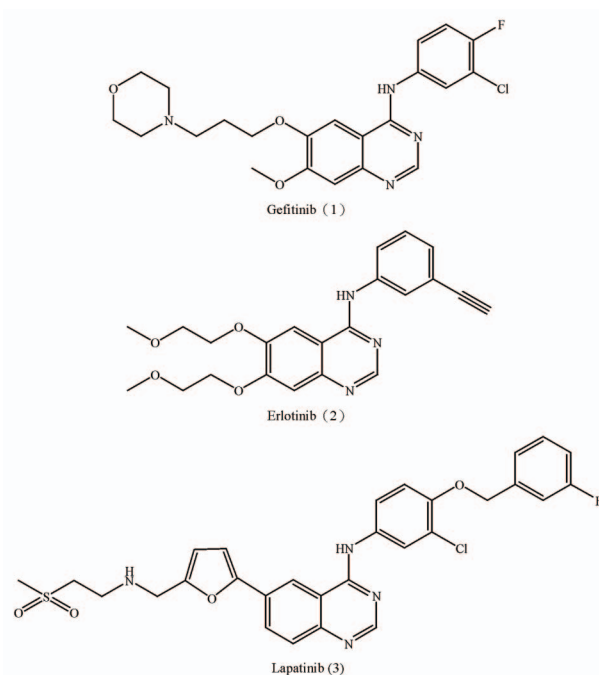


Fig. 1. EGFR receptor tyrosine kinase inhibitors in clinical use.

Dedicated to Professor Ho-Hsiang Wei on the occasion of his 70<sup>th</sup> birthday.

\* Corresponding author. B.-C. Wang, Tel: +886-2-26215656 ext. 2438; E-mail: bcw@mail.tku.edu.tw;

L.-L. Yang, Tel: +886-2-27361661; E-mail: llyang@tmu.edu.tw

be used for the clinical trial of breast cancer.<sup>5</sup> These agents belong to the 4-anilinoquinazoline class and the key features between the receptor have been revealed. Over the years, compounds belonging to 4-anilinoquinazoline family are reported to be useful as an analgesic and anti-inflammatory agent and used in the treatment of cancer. A major step forwarded in the development of EGFR-targeted drugs was the discovery of the high inhibitory ability of the 4-[(3-bromophenyl) amino]-quinazoline.<sup>6</sup> Nowadays, a number of reports have been presented that a broad class of 4-anilinoquinazolines are potent and highly selective inhibitors of EGF-R phosphorylation, resulting from the competitive binding at the ATP (Adenosine triphosphate) site. Since the 4-anilinoquinazoline class of inhibitors has been discovered to be effective, there is a great demand to employ the distinctive structure-activity relationship (SAR) models for a broad class of 4-anilino quinazolines to investigate their abilities to inhibit EGFR autophosphorylation.<sup>7,8</sup>

Computer-assisted drug design (CADD) represents the more recent applications of computers as tools in the drug design process. The success of CADD should depend upon the amount of information that is available about the ligand and receptor.<sup>9</sup> Based on the information that is available, one can apply either ligand-based or receptor-based molecular design methods to find interesting lead molecules quickly. The results can be used to predict biological activities of untested molecules, propose compounds for synthesis, validate models of receptor binding sites, and optimize pharmacokinetic properties of compounds. The ligand-based approach is applicable when the structure of the receptor is unknown. When a series of compounds have been identified that can exert the activity of interest, and the quantitative structure-activity relationships (QSAR) would become an alternative powerful theoretical tool for the description and prediction of properties of complex molecular systems in different environments.<sup>10-13</sup>

The ultimate goal of CADD is to determine interesting lead molecules which are worth for further drug research and synthesis by the related laboratory. The factors which affect the protein-ligand interactions can be characterized by using different QSAR methods or molecular docking programs.<sup>14-18</sup> Pharmacophore modeling is one of the best 3D-QSAR methods that has been widely used for generating the chemical features of relative compounds.<sup>19-21</sup> The method based on 3D structural information of molecules, and has been successfully applied to the

drug discovery. For the numerous therapeutically relevant drug targets with undetermined active site geometries, pharmacophore modeling has shown to provide an effective mechanism for virtual screening. In this study, pharmacophore methodologies are used to establish a correlation between chemical structure and specific biological activity, the method has been demonstrated as an effective tool in discovering novel lead compounds.

The purpose of the present work is to establish a pharmacophore model for the inhibition of Tyrosine Kinase that could serve as a guide for the rational design of high potent and selective inhibitors. We focus on the concept of 3D pharmacophores in the context of similarity assessments. A pharmacophore is based on the concept that specific interactions are observed in the drug and receptor interactions. In order to rapidly identify the new potential drugs, it is expected that the established pharmacophore models are able to correctly elucidate the QSAR of the tyrosine kinase inhibitors.

## MATERIALS AND METHODS

### Biological data

The parent compound of Tyrosine Kinase inhibitor "4-anilinequinazoline" contains quinazoline and aniline segments (Fig. 2). According to the geometrical analysis,

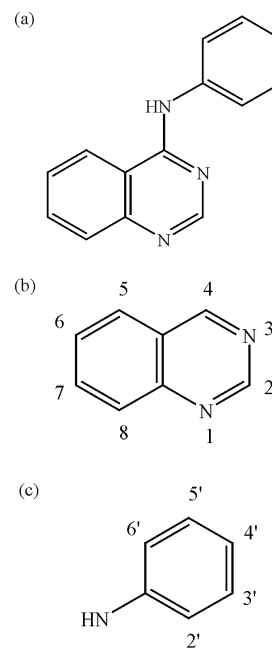


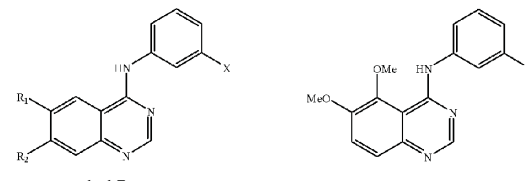
Fig. 2. Structure of: (a) 4-anilinequinazoline; (b) quinazoline; (c) aniline.

quinazoline is made up of two fused six-membered aromatic rings; a nitrogen atom connects two electron-rich groups through two rotatable N-C single bonds. The dihedral angle between the aniline and quinazoline should be treated with caution. Table 1 shows the chemical structures of 4-anilinoquinazoline derivatives. Medicinally, quinazoline-like compounds could be used in various areas especially in anti-malarial agent and cancer treatment.<sup>22</sup> The tyrosine kinase activities of the epidermal growth factor receptor which are represented as  $IC_{50}$  in nM, were obtained from the literature data.<sup>6</sup> All the initial inhibition activities were divided into five levels, and three compounds were selected from each level to perform the pre-analysis. The compounds of training and test sets were selected by considering the fact that test set compounds represent a range of biological activity and chemical classes similar to that of the training sets. The selection of a suitable training set is critical for the quality of pharmacophore models as generated automatically. To ensure the statistic relevance of the calculated model, the training set should contain a set of diverse compounds and their activity data. These should spread over 4-5 orders of magnitude equally and are originated from the comparable binding assays. Each selected compound should add new information to the model while avoiding redundancy and bias both in terms of structural features and activity range.<sup>19</sup> In Table 1, all of the training set compounds are presented as the 2D chemical structures, the most potent inhibitor shows an  $IC_{50}$  of 0.025 nM and exhibits the least value of 12,000. Due to the pharmacophore modeling needed, the most active compounds should provide information on the most critical feature. Thus, on the basis of the above criteria, 16 compounds for the training set and 9 compounds for the test set were selected.

### Pharmacophore modeling

A pharmacophore is defined as the 3D structural features that illustrate how a ligand molecule can interact with a target receptor in a specific binding site. When the asset of active ligands is available, it is possible to compute their shares of pharmacophore.<sup>20,21</sup> In particular, pharmacophore model in Discovery Studio 2.1 is generally referred to as a 'hypothesis' which consists of a collection of features necessary for the biological activity of the ligands oriented in 3D space. In order to generate a pharmacophore, all molecules (both training and test sets) should be built and minimized within the Discovery Studio 2.1 software.<sup>15</sup> Conformation models for all of the molecules were generated by

Table 1. Structure of 4-anilinoquinazoline class of inhibitors and relative  $IC_{50}$



No.	R <sub>1</sub>	R <sub>2</sub>	X	$IC_{50}$ (nM)
1	H	H	CF <sub>3</sub>	577.000
2	NO <sub>2</sub>	H	H	5000.000
3	NO <sub>2</sub>	H	Br	900.000
4	H	OMe	Br	10.000
5	H	NH <sub>2</sub>	H	100.000
6	H	NH <sub>2</sub>	F	2.000
7	H	NH <sub>2</sub>	I	0.350
8	H	NO <sub>2</sub>	H	12000.000
9	H	NO <sub>2</sub>	F	6100.000
10	OMe	OMe	Br	0.025
11	OMe	OMe	I	0.890
12	NMe <sub>2</sub>	H	Br	84.000
13	H	OH	Br	4.7000
14	H	NHAc	Br	40.000
15	H	NHMe	Br	7.000
16	5,6-diOMe			1367.000

using the CHARMM force field parameters and a constraint of 20 kcal/mol energy thresholds above the global energy minimum.<sup>23</sup> Discovery Studio 2.1 selects conformers using the Poling algorithm, that penalizes any newly generated conformer which is too close to an already formed conformer in the set.<sup>24</sup> This method ensures maximum coverage in conformational space. All other parameters were set to the default settings.

The resulting hypotheses are specified as several default feature types (e.g. hydrogen bond acceptor, hydrogen bond donor, hydrophobic, ring aromatic, negative/positive ionizable) located at the well-defined positions (location constraints). These are surrounded by certain spatial tolerance spheres, designating the area in space to be occupied by the corresponding chemical functions of the matched molecule. Each of the features is assigned a certain weight that is proportional to its relative contribution to the biological activity. Hydrogen bond acceptors/donors, and aromatic rings include an additional vector, defining the direction of the interaction. The results of the hypotheses include different statistical values calculated during the model generation, and the best model should be selected on the basis of the lowest total cost, rms values and high corre-

Table 2. Results obtained from pharmacophore hypothesis generation using the training set molecules<sup>a</sup>

Hypo number	Total cost	rms	Correlation	Features <sup>b</sup>
1	73.81	0.98	0.95	HBD, HYD, aliHYD, aroHYD
2	74.11	0.97	0.96	HBD, HYD, aliHYD, HYD
3	74.30	1.01	0.95	HBD, HYD, aroHYD, HYD
4	75.49	0.93	0.96	HBD, HYD, HYD, HYD
5	82.00	1.41	0.90	HBD, HYD, aliHYD HYD, R A
6	82.92	1.44	0.90	HBD, HYD, alipHYD, aroHYD, R A
7	89.90	1.76	0.84	HBD, HYD, alipHYD, alipHYD, aroHYD
8	95.36	2.05	0.78	HBD, HYD, R A
9	95.89	2.22	0.71	HYD, HYD, HYD, HYD
10	96.24	2.21	0.71	HBD, HYD, HYD, HYD, HYD

<sup>a</sup> Null cost = 123.97 and Fixed cost = 58.67. All costs are in units of bits.<sup>b</sup> HBD (hydrogen bond donor), HYD (hydrophobic, ali = aliphatic, aro = aromatic) and RA (ring aromatic).

lation of the 3D arrangement of features with their corresponding pharmacological activities in a given set of training compounds.

## RESULTS AND DISCUSSION

There are several methods for generating 3D QSAR models. Several 3D QSAR studies of quinazoline type EGF-R inhibitors have been reported.<sup>12,25</sup> In one example, the steric and electrostatic fields were computed, and correlated with the activity (e.g. CoMFA, CoMSIA).<sup>26</sup> The results for the ligand-based design indicated that the electron-withdrawing lipophilic substituents on the 3'-position of the aniline are favorable, and electron-donating groups at the 6- and 7-position of the quinazoline are preferred.

However, CoMFA or CoMSIA is incapable of describing appropriately all binding forces, because the method is based only on standard steric and electrostatic molecular fields to model receptor-ligand interactions. In Discovery Studio, 3D QSAR models are generated and based on how well a series of ligands fit in a pharmacophore. The better a ligand fits a pharmacophore (e.g. the more features that map and the closer they are to the feature centroids), the more active it is predicted to be. To assess the significance of the receptor-ligand interaction, we presented an evaluation of the cross-validation for the pharmacophore results and used LibDock protocol for the docking of ligands into the binding pocket of EGFR.<sup>27</sup>

### Pharmacophore Generation & Assessment

3D QSARs differ from typical QSAR methods in that the descriptors are derived from ligand alignments or how well ligands fit a pharmacophore, rather than the molecular

features. Often, the descriptors are concerned with the overall molecule instead of a single substituent. In Discovery Studio, 3D QSAR models are generated and based on how well a series of ligands fit a pharmacophore. The better a ligand fits a pharmacophore (i.e., the more features that map and the closer they are to the feature centroids), the more active it is predicted to be.

Since the Pharmacophore Generation protocol can only generate a maximum of five features for a hypothesis. An initial analysis of the "show function mapping" tools revealed that hydrogen bond acceptor (HBA), hydrogen bond donor (HBD), hydrophobic (HYD), and ring aromatic (RA) features could effectively map all the critical chemical/structural features of all the training set molecules. Therefore, these features were used to generate 10 pharmacophore hypotheses from the training set, using a default uncertainty value of 3. The uncertainty value represents a ratio range of uncertainty in the activity value based on the expected statistical irregularities of biological data collected.

The quantitative models were generated for the sixteen compounds in the training set (compound **1-16**, Table 1). Table 2 lists the top 10 hypothesis generated by HypoRefine algorithm together with their statistical parameters. As shown in Fig. 3, the best hypothesis Hypo1 contains three features, including one hydrogen-bond acceptor (A), and three hydrophobic features (including aliphatic and aromatic). The main difference between Hypo1 and Hypo2 was the addition of excluded volume. Although Hypo2 has slight improvement in the rms value, Hypo1 comprehends two excluded volume (E) which exhibit the significant meaning of actual ligand-protein inter-

actions. Besides, Hypo1 was characterized by the good correlation coefficient (0.95), the lowest total cost value (73.81), and the acceptable rms (0.98).

### Validation of Pharmacophores

Ideally, a good pharmacophore model should not only be able to predict the activities of the training set compounds accurately, but also can predict the activities of external compounds of test set.<sup>28</sup> To further validate our design rationale, cross-validation methods were used for assessing the performance of the generated pharmacophore models. For the use of test set method, nine compounds with different bioactivities represented as ( $-\log IC_{50}$ ) and structures were selected to form a test set. Discovery Studio 2.1/Ligand Pharmacophore Mapping protocol was used with Hypo 1 as pharmacophore model to screen the designed database. All of the test set compounds were prepared by using the same method as that for the training set, and the model analysis has resulted in the unique model with a cross-validated coefficient of 0.762 (Fig. 4). Further attempts were also made to classify the real screening results to the active and inactive compounds by applying the pharmacophore model. For this purpose, the activity values of the training set compounds were classified into three categories: highly active ( $IC_{50} \leq 50$  nM, +++), moderately active ( $50 < \text{nM } IC_{50} \leq 1000$  nM, ++), and low active ( $IC_{50} > 1000$  nM, +). Table 3 shows the predicted and experimental inhibitory activities of these 16 molecules in the training set. This classification scheme is shown to be more consequential than the actual prediction values.

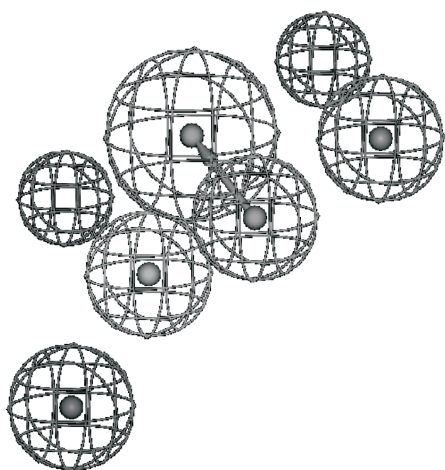


Fig. 3. HipHop model generated by compounds (1-16) in the training set (Hypo1).

### Docking Study

Protein-ligand docking software is widely used to promote the drug design that has the potential to identify the promising lead compounds at an early stage of the drug discovery pipeline.<sup>29-31</sup> LibDock is based on matching the polar and apolar binding site features of the protein-ligand complex, and this algorithm was developed by Diller and Merz.<sup>32</sup> The algorithm uses protein site features referred to as HotSpots which consist of polar and apolar types. Polar Hotspot is preferred by a polar ligand atom (e.g. a hydrogen

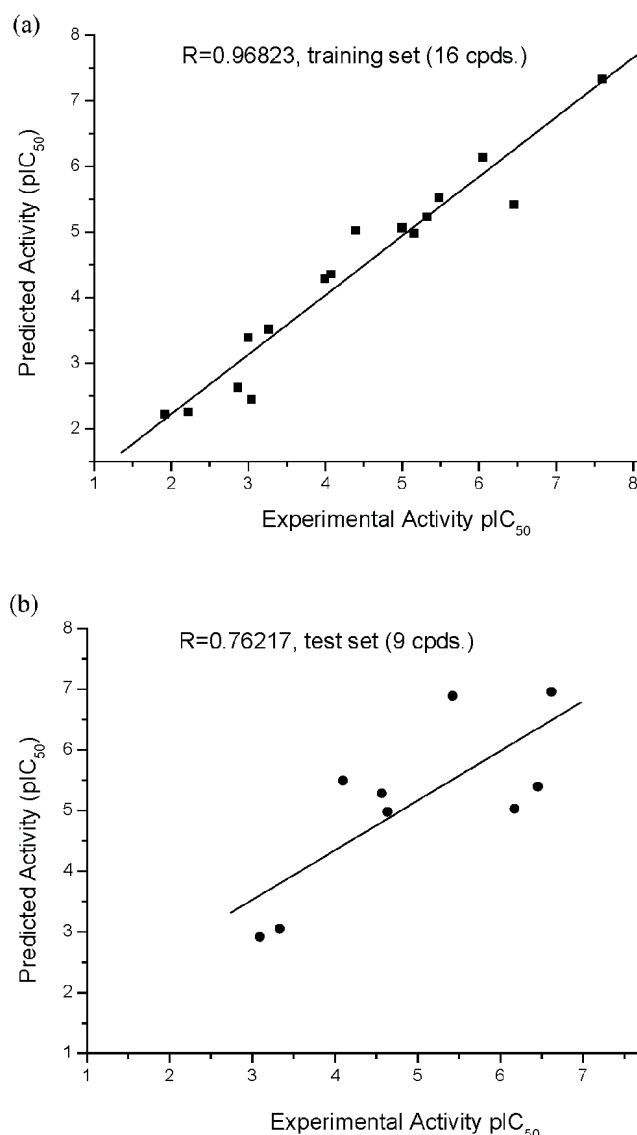


Fig. 4. Plot of the correlation between the experimental and predicted activities (by using Hypo1) for the (a) Training set and (b) Test set compounds.



Table 3. Experimental and predicted activities (using Hypo1) of the training set compounds

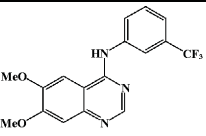
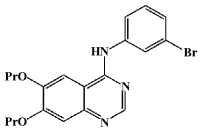
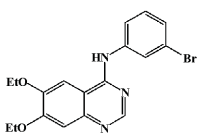
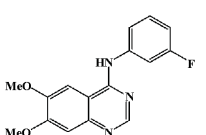
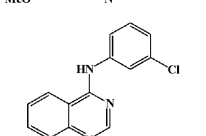
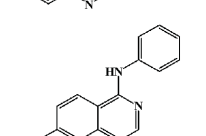
Compound No.	Experimental IC <sub>50</sub> (nm)	Predicted IC <sub>50</sub> (nm)	Error <sup>a</sup>	Fit value <sup>b</sup>	Experimental scale <sup>c</sup>	Predicted scale <sup>c</sup>
1	0.025	0.046	+1.84	10.43	+++	+++
2	0.890	0.726	-1.23	10.42	+++	+++
3	3.300	2.993	-1.10	8.83	+++	+++
4	0.350	3.784	+10.81	8.67	+++	+++
5	4.700	5.869	+1.25	8.47	+++	+++
6	10.000	8.614	-1.16	8.29	+++	+++
7	40.000	9.469	-4.22	8.25	+++	+++
8	7.000	10.440	+1.49	8.21	+++	+++
9	84.000	44.197	-1.90	7.99	++	+++
10	100.000	51.566	-1.94	7.08	++	++
11	540.000	302.742	-1.78	6.95	++	++
12	1000.000	406.343	-2.43	6.86	++	++
13	1367.000	2332.250	+1.71	6.68	+	+
14	900.000	3569.360	+3.97	6.60	++	+
15	6000.000	5482.320	-1.09	5.84	+	+
16	12000.000	6023.580	-1.99	5.77	+	+

<sup>a</sup> A ratio between the experimental and predicted activities. A positive value indicates that the predicted IC<sub>50</sub> is lower than the experimental IC<sub>50</sub>.

<sup>b</sup> Fit value indicates how well the features in the hypothesis overlap the chemical features in the compound.

<sup>c</sup> Activity scale: +++, IC<sub>50</sub> ≤ 50 nM (highly active); ++, 50 nM < IC<sub>50</sub> ≤ 1000 nM (moderately active); +, IC<sub>50</sub> > 1000 nM (low active).

Table 4. Results of LibDock docking score and corresponding experimental value

Compound No	Structure	LibDock docking score	Experimental IC <sub>50</sub> (nm)
T1		123.403	0.240
T2		120.193	0.170
T3		113.551	0.006
T4		109.456	3.800
T5		100.118	23.000
T6		98.265	12000.000

bond donor or acceptor) and an apolar HotSpot is preferred by an apolar atom (e.g. a carbon atom). The receptor HotSpot file was calculated prior to the docking procedure. The following docking study was carried out by LibDock within Discovery Studio 2.1 package (Accelrys, San Diego, U.S.A.), and the Dreiding force field was used for all calculations. The docking and subsequent scoring were performed by using default parameters, where the X-ray structure of EGFR-R in complex with a POX inhibitor were obtained from the Brookhaven Protein Data Bank (PDB code: 3BEL1). The binding site of the bound ligand (POX, 4-amino-6-{{[1-(3-fluorobenzyl)-1H-indazol-5-yl]amino}-pyrimidine-5-carbaldehyde O-(2-methoxyethyl)oxime}) was identified as the active site, and the solvent molecules far away the active site were removed (Fig. 5).

The binding modes of the quinazoline type inhibitors at the ATP binding site of EGF-R have been reported by several groups.<sup>1</sup> The nitrogen atom connects both aniline and quinazoline groups, and the direction of the hydrogen bond acceptor is vital for the inhibitory activity. The SAR at the oxime side chain (R2 group) has been reported to have a negative effect against activity.<sup>25</sup> In this work, we focus our attention on the surrounding of each pharmacophore features. The results show that compounds with hydrophobic substituents at 6 and 7 positions of the quinazoline are more potent in the experimental assay. This observation is also in agreement with the pharmacophore

model. In Fig. 6, the substituent at 3'-position of aniline occupies a pocket formed by the side chains of Met766, Leu777, Thr790, Thr854, and Phe856 (Fig. 6a, 6b). Electron-withdrawing lipophilic substituents on the 3-position of the aniline are favorable, especially the chlorine and bromine groups give the optimal effect. Both the steric effect and intra-molecular hydrogen bond favor the inhibitory activity, such phenomenon is revealed in Fig. 5. The replacement by trifluoromethyl group may further enhance the hydrogen bond formation among the residues. Moreover, the electron-donating groups at R1 position of the quinazoline are preferred.

### Molecular surface comparison

The study of molecular surface is an important analysis of geometry, it can be used for the exploration of a protein folding, docking, and interactions between proteins. Various physical chemical properties can be mapped onto the molecular surface. To further validate our design rationale, we compared the shape of the highest activity compound T1 and POX (Fig. 7a, 7b), and the higher score compounds were shown to have similar orientation lying on the active site position. According to the docking results, three compounds (T1, T2, and T3) exhibited high scores that have the same backbone near the free NH linker, and the torsion angle defined by aniline and pyrimidine is around 100 degree (Fig. 7c). The hydrophobicity of aliphatic feature suggests that alkyl chain at the C-7 position is an important hint. This assumption agrees well with the structure

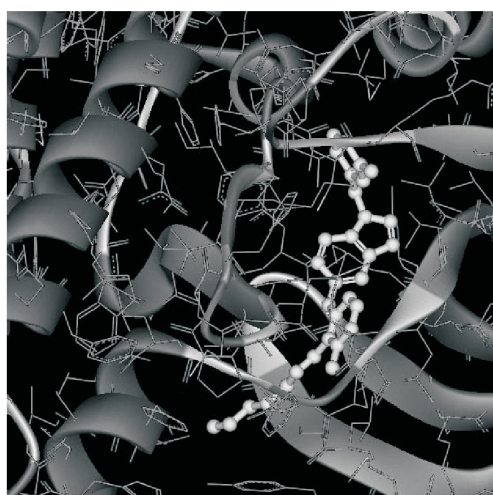


Fig. 5. Stereoview for comparative binding affinities of POX (yellow, ball and stick).

surface of POX.

The results from the above structural analysis of protein-ligand relationship provide the explanation of the binding modes which were shown to fit the pharmacophore model and the docking results. The amino modes around anilino group form extra intramolecular hydrogen bonds, and the overall molecular surface should fit the molecule shape as well as the POX inhibitor.

### CONCLUSIONS

A pharmacophore modeling, containing HipHop and HypoRefine modules within Discovery Studio 2.1 software package, was used to elucidate the structure-activity relationship of tyrosine kinase inhibitors. The pharmacophore model Hypo1 was shown to give the best quantitative results with a high correlation coefficient (0.968), and possess the best predictive power (cross-validation correlation coefficient of 0.762). The results on docking scores provide information on the geometry of the binding site cavity

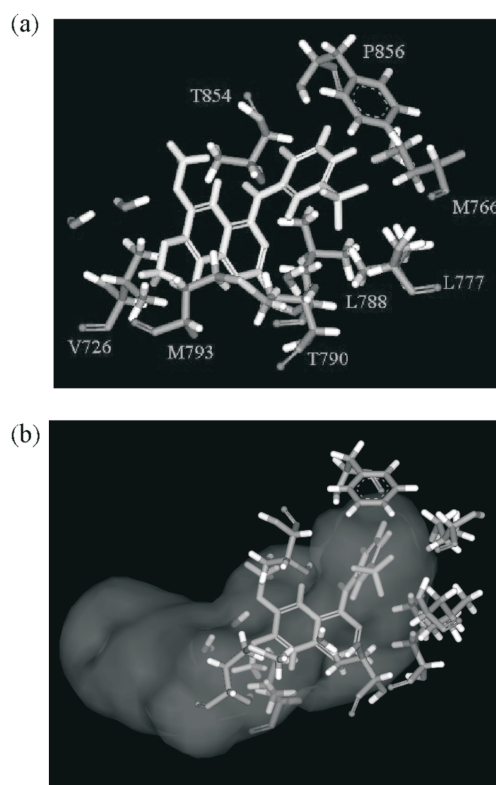


Fig. 6. (a) Complexed structure of docking result: compound T1 and protein residues are colored as yellow and green, respectively. (b) Molecular surface is created by POX inhibitor.

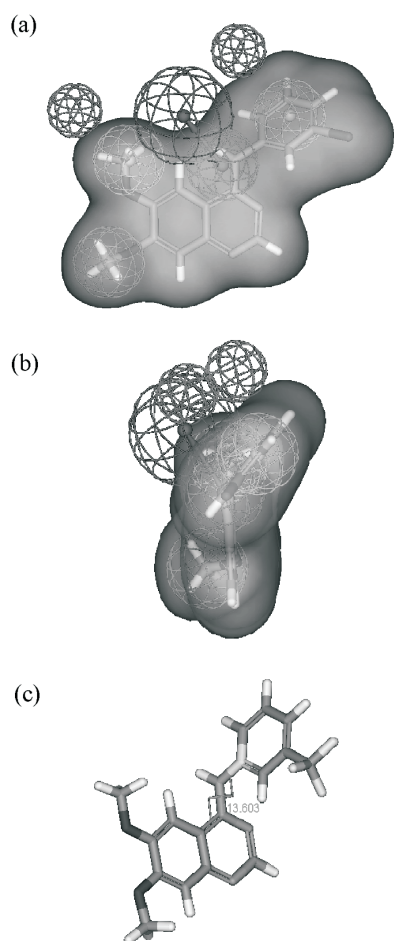


Fig. 7. (a) Pharmacophore model Hypo1 mapped to the most active compound (10,  $IC_{50}$  = 0.025 nM); (b) Stereoview for structure surface; (c) Torsion angle between anilino and quinazoline group.

and the relative substituents of various properties in different site pockets for each of the substrates considered. Finally, the molecular surface structure of quinazoline type inhibitor with EGFR together with the pharmacophore mapping from the software offer well interpretation on the structure activities of the inhibitors and afford us important information for protein-ligand relationship.

#### ACKNOWLEDGEMENT

We gratefully acknowledge the National Council Science of Taiwan for financial support of this work (Grant No. 98-2113-M-032-004-MY3), and especially thank Professor Chhiu-Tsu, Lin (Northern Illinois University) for giving some amendment of English grammar.

Received January 5, 2010.

#### REFERENCES

1. Wissner, A.; Berger, D. M.; Boschelli, D. H.; Floyd, Jr., M. B.; Greenburger, L. M.; Gruber, B. C.; Johnson, B. D.; Mamuya, N.; Nilakantan, R.; Reich, M. F.; Shen, R.; Tsou, H. R.; Upešlacis, E.; Wang, Y. F.; Wu, B.; Ye, F.; Zhang, N. *J. Med. Chem.* **2000**, *43*, 3244-3256.
2. Chandregowda, V.; Kush, A. K.; Chandrasekara Reddy, G. E. *J. Med. Chem.* **2009**, *44*, 3046-3055.
3. Chen, W. F.; Wong, M. S. *J. Clin. Endocrinol. Metab.* **2004**, *89*(5), 2351-2359.
4. Talapatra, S.; Thompson, C. B. *J. Pharmacol. Exp. Ther.* **2001**, *298*(3), 873-878.
5. Xu, G.; Searle, L. L.; Hughes, T. V.; Beck, A. K.; Connolly, P. J.; Abad, M. C.; Neeper, M. P.; Struble, G. T.; Springer, B. A.; Emanuel, S. L.; Gruninger, R. H.; Pandey, N.; Adams, M.; Moreno-Mazza, S.; Fuentes-Pesquera, A. R.; Middleton, S. A.; Greenberger, L. M. *Bioorg. Med. Chem. Lett.* **2008**, *18*, 3495-3499.
6. Bridges, A. J.; Zhou, H.; Cody, D. R.; Rewcastle, G. W.; McMichael, A.; Showalter, H. D. H.; Fry, D. W.; Kraker, A. J.; Denny, W. A. *J. Med. Chem.* **1996**, *39*, 267-276.
7. Rewcastle, G. W.; Palmer, B. D.; Bridges, A. J.; Showalter, H. D. H.; Sun, L.; Nelson, J.; McMichael, A.; Kraker, A. J.; Fry, D. W.; Denny, W. A. *J. Med. Chem.* **1996**, *39*, 918-928.
8. Rewcastle, G. W.; Palmer, B. D.; Thompson, A. M.; Bridges, A. J.; Cody, D. R.; Zhou, H.; Fry, D. W.; McMichael, A.; Denny, W. A. *J. Med. Chem.* **1996**, *39*, 1823-1835.
9. Khandelwal, A.; Krasowski, M. D.; Reschly, E. J.; Sinz, M. W.; Swaan, P. W.; Ekins, S. *Chem. Res. Toxicol.* **2008**, *21*, 1457-1467.
10. Tsai, K. C.; Lin, T. H. *J. Chem. Inf. Comput. Sci.* **2004**, *44*, 1857-1871.
11. Liao, H. R.; Chang, Y. S.; Lin, Y. C.; Yang, L. L.; Chou, Y. M.; Wang, B. C. *J. Chin. Chem. Soc.* **2006**, *53*, 1251-1261.
12. Bursi, R.; Sawa, M.; Hiramatsu, Y.; Kondo, H. *J. Med. Chem.* **2002**, *45*, 781-788.
13. Hevener, K. E.; Ball, D. M.; Buolamwini, J. K.; Lee, R. E. *Bioorg. Med. Chem.* **2008**, *16*, 8042-8053.
14. Huang, Z.; Wong, C. F. *J. Phys. Chem. B* **2009**, *113*, 14343-14354.
15. Shrestha, A. R.; Shindo, T.; Ashida, N.; Nagamatsu, T. *Bioorg. Med. Chem.* **2008**, *16*, 8685-8696.
16. Hartshorn, M. J.; Verdonk, M. L.; Chessari, G.; Brewerton, S. C.; Mooij, W. T. M.; Mortenson, P. N.; Murray, C. W. *J. Med. Chem.* **2007**, *50*, 726-741.
17. Tiwari, R.; Mahasenan, K.; Palvovicz, R.; Li, C.; Tjarks, W. *J. Chem. Inf. Model.* **2009**, *49*, 1581-1589.
18. Costanz, S. *J. Med. Chem.* **2008**, *51*, 2907-2914.
19. Singh, N.; Nolan, T. L.; McCurdy, C. R. *J. Mol. Graph. Mod.*



- 2008, 27, 131-139.
20. Chen, J. H.; Liu, T. L.; Yang, L. J.; Li, L. L.; Wei, Y. Q.; Yang, S. Y. *Chem. Pharm. Bull.* **2009**, 57(7), 704-709.
21. Huang, W. H.; Yu, H. P.; Sheng, R.; Li, J.; Hu, Y. Z. *Bioorg. Med. Chem.* **2008**, 16, 10190-10197.
22. Rewcastle, G. W.; Murray, D. K.; Elliott, W. L.; Fry, D. W.; Howard, C. T.; Nelson, J. M.; Roberts, B. J.; Vincent, P. W.; Showalter, H. D. H.; Winters, R. T.; Denny, W. A. *J. Med. Chem.* **1998**, 41, 742-751.
23. Brooks, B. R.; Bruccoleri, R. E.; Olafson, B. D.; States, D. J.; Swaminathan, S.; Karplus, M. *J. Comput. Chem.* **1983**, 4, 187-217.
24. Smellie, A.; Teig, S. L.; Towbin, P. *J. Comput. Chem.* **1995**, 16, 171-187.
25. Hou, T. J.; Zhu, L. L.; Chen, L. R.; Xu, X. J. *J. Chem. Inf. Comput. Sci.* **2003**, 43, 273-287.
26. Cramer, R. D., III.; Patterson, D. E.; Bunce, J. D. *J. Am. Chem. Soc.* **1988**, 110, 5959-5967.
27. Rao, S. N.; Head, M. S.; Kulkarni, A.; LaLonde, J. M. *J. Chem. Inf. Model.* **2007**, 47, 2159-2171.
28. Singh, N.; Chevé, G.; Ferguson, D. M.; McCurdy, C. R. *J. Comput. Mol. Des.* **2006**, 20, 471-493.
29. Ragno, R.; Frasca, S.; Manetti, F.; Brizzi, A.; Massa, S. *J. Med. Chem.* **2005**, 48, 200-212.
30. Ferrari, A. M.; Wei, B. Q.; Costantino, L.; Shoichet, B. K. *J. Med. Chem.* **2004**, 47, 5076-5084.
31. Corbeil, C. R.; Englebienne, P.; Yannopoulos, C. G.; Chan, L.; Das, S. K.; Bilimoria, D.; L'Heureux, L.; Moitessier, N. *J. Chem. Inf. Model.* **2008**, 48, 902-909.
32. Diller, D. J.; Merz, Jr., K. M. *Proteins* **2001**, 43, 113-124.